

# The formation of Co<sub>2</sub>C species in activated carbon supported cobalt-based catalysts and its impact on Fischer–Tropsch reaction

Jianmin Xiong<sup>a</sup>, Yunjie Ding<sup>a,b,\*</sup>, Tao Wang<sup>a</sup>, Li Yan<sup>a</sup>, Weimiao Chen<sup>a</sup>, Hejun Zhu<sup>a</sup>, and Yuan Lu<sup>a</sup>

<sup>a</sup>Natural Gas Utilization and Applied Catalysis Laboratory, Dalian Institute of Chemical Physics, Chinese Academy of Sciences, Dalian, 116023, China

<sup>b</sup>State Key Laboratory of Catalysis, Dalian Institute of Chemical Physics, Chinese Academy of Sciences, Dalian, 116023, China

Received 17 March 2005; accepted 19 April 2005

The cobalt carbide (Co<sub>2</sub>C) species was formed in some activated carbon supported cobalt-based (Co/AC) catalysts during the activation of catalysts. It was found that the activity of Fischer–Tropsch reaction over Co-based catalysts decreased due to the formation of cobalt carbide species. Some promoters and pretreatment of activated carbon with steam could restrain the formation of cobalt carbide.

**KEY WORDS:** cobalt carbide species; Fischer–Tropsch synthesis; cobalt-based catalysts; activated carbon.

## 1. Introduction

Fischer–Tropsch synthesis (FTS) is a most important way to synthesize clean, high quality oil fraction without sulphur from coal or natural gas and it is boomed by energy crisis and environment protection [1,2]. Cobalt-based catalyst is considered to be good catalysts for FTS because of its high activity, high stability, relatively low cost and low water shift reaction [3,4]. To enhance the activity of cobalt catalysts the active compound precursors were dispersed on porous carriers with SiO<sub>2</sub>, Al<sub>2</sub>O<sub>3</sub> and TiO<sub>2</sub> being the most frequently used. The interaction between cobalt and the supports leads to the formation of Co-support compounds including Co<sub>2</sub>SiO<sub>4</sub>, CoAl<sub>2</sub>O<sub>4</sub> and CoTiO<sub>3</sub> compounds, which can be only reduced or decomposed at elevated temperatures (>1000 K), and declines the activity of catalysts in FTS [5–9].

There are a few studies worked on the cobalt-based catalysts supported on activated carbon for FTS [10–13], but few research figures out whether there is Co-support compound existing in activated carbon supported cobalt-based catalysts and points out its impacts on the performance of F–T reaction. We studied the property of activated carbon supported cobalt-based (Co/AC) catalysts in FTS previously, and found that the catalyst had restricted chain producibility, the products of FTS major in naphtha and diesel distillates [14,15]. Our previous studies indicated that the doping of ZrO<sub>2</sub> could increase CO conversion, detract the formation of methane and enhance the selectivity of long chain products over the Co/AC catalysts [16,17].

This paper presents the performance of potassium, manganese, chromium-promoted Co/AC catalysts and a

catalyst made from steam-pretreated activated carbon at high temperature. The aim of this paper will investigate the formation of the Co<sub>2</sub>C species in some Co/AC catalyst and its impacts on the catalytic behaviors of CO hydrogenation over Co-based catalysts.

## 2. Experimental

### 2.1. Catalysts preparation

The activated carbon used in this study was made from almond materials. Steam pretreatment of the activated carbon was conducted with steam for 3 h at 1123 K. Co(NO<sub>3</sub>)<sub>2</sub>·6H<sub>2</sub>O (AR) used as the precursor of cobalt, KNO<sub>3</sub> (AR), Mn(NO<sub>3</sub>)<sub>2</sub> (50% solution) and Cr(NO<sub>3</sub>)<sub>3</sub>·9H<sub>2</sub>O (AR) used as the precursors of promoters, respectively. The catalysts were prepared by aqueous incipient wetness co-impregnation of activated carbon with aqueous solutions of cobalt nitrate and with or without the solution of promoter precursor, with the amount of cobalt to be 15% by weight. The wet samples were dried at room temperature for several days, then baked at 363 K for 2 h in air and finally at 473 K for 8 h under pure N<sub>2</sub>. The catalysts with and without co-impregnated promoters were denoted as 15CoXM/AC (X: the amount of promoter by weight, M = K, Mn, Cr) and 15Co/AC, respectively. The catalyst made from the steam-pretreated activated carbon was denoted as 15Co/AC-S.

### 2.2. Fischer–Tropsch reaction

The testing apparatus consisted of a fixed bed tubular reactor with an external heating system. The reactor was made of stainless steel with 350 mm length, 10 mm inner diameter. The catalysts were *in situ* activated in a flow of

\*To whom correspondence should be addressed.

E-mail: dyj@dicp.ac.cn

H<sub>2</sub> at 623 K for 19 h before CO hydrogenation. Then the syngas (H<sub>2</sub>/CO=2) was fed into the catalyst bed under conditions of 503 K, 2.5 MPa and GHSV = 500 h<sup>-1</sup>. The effluent passed through a high-pressure gas-liquid separator that inserted in an ice-water bath. After 25 h stabilization, the liquid products for another 50 h were off-line analysed by HP-6890 GC with an HP-5 (cross linked 5% PH ME siloxane) capillary column and FID detector. The tail gas was on-line analyzed by HP-6890 GC with a Porapack-Q column and TCD detector.

### 2.3. Catalysts characterization

All the used samples were washed with CS<sub>2</sub> solution before characterization in order to clean the produced liquid products in the catalysts. The catalyst of 15Co/AC without FTS reaction, which was activated under the same condition with the same procedures and then passivated in air, was denoted as 15Co/AC-P. The X-ray diffraction (XRD) patterns of catalysts were conducted in air on X' Pert PRO diffractometer (PANalytical) using CuK<sub>α1</sub> radiation at 40 kV and 40 mA and were recorded from 35° to 60° at a scanning rate of 0.02°/s. The particle sizes of cobalt particles were calculated by the Scherer equation using cubic cobalt [111]:  $d = B\lambda/\beta_{1/2}\cos\theta$  where  $\lambda$  is the X-ray wavelength,  $B$  is the particle shape factor, and  $\beta_{1/2}$  is the full width at half-maximum (in radians) of the cobalt line.

X-ray photoelectron spectroscopy (XPS) measurement was performed using a VG ESCA LABMK II spectrometer. The instrument typically operated at pressure below  $1.33 \times 10^{-7}$  Pa and AlK<sub>α</sub> line (1486.6 eV) was used. The binding energy of all spectra was calibrated with respect to the C<sub>1s</sub> line at 284.6 eV.

## 3. Results and discussion

### 3.1. Performance of Fischer–Tropsch reaction

Table 1 shows the performance of Fischer–Tropsch reaction over various Co/AC catalysts. The FTS activity of 15Co/AC-S was the highest in all catalysts (ca. 62.2 mmol CO g Co<sup>-1</sup> h<sup>-1</sup>), and the selectivity of C<sub>5</sub><sup>+</sup> could reach ca. 73.2%. Comparing with data of 15Co/AC catalysts, it could be concluded that the pre-treatment of activated carbon with steam at high temperature could greatly enhance CO hydrogenation activity of Co-based catalyst. However, the activity decreased from 28.4 to 10.6 mmol CO g Co<sup>-1</sup> h<sup>-1</sup> and the selectivity of CH<sub>4</sub> increased from 13.9% to 34.4% when 1.0 wt.% K was doped on 15Co/AC catalysts.

It is interesting to find that the activity of F–T reaction first decreased from 28.4 to 20.2 mmol CO g Co<sup>-1</sup> h<sup>-1</sup>, and the selectivity of CH<sub>4</sub> decreased from 13.9% to 5.9% when 1 wt.% Mn were added into Co/AC catalysts, then the activity increased surprisingly when

Table 1  
The catalytic behavior of Fischer–Tropsch reaction over various Co/AC catalysts

Catalysts	Activity mmol g Co <sup>-1</sup> h <sup>-1</sup>	Selectivity, mol.%		
		Methane	C <sub>2</sub> -C <sub>4</sub>	C <sub>5</sub> <sup>+</sup>
15Co/AC	28.4	13.9	20.7	62.0
15Co/AC-S	62.2	14.8	11.9	73.2
15Co1K/AC	10.6	34.4	24.4	39.4
15Co1Mn/AC	20.2	5.9	14.0	80.0
15Co3Mr/AC	39.2	18.4	20.1	61.3
15Co5Mn/AC	50.9	27.3	19.7	52.9
15Co1Cr/AC	50.2	18.3	16.8	64.7
15Co3Cr/AC	58.6	20.9	16.3	62.7
15Co5Cr/AC	56.3	20.6	15.0	64.3
15Co7Cr/AC	54.5	27.8	14.8	55.8

Reaction conditions:  $T = 503$  K, 2.5 MPa, H<sub>2</sub>/CO=2 and GHSV = 500 h<sup>-1</sup>.

more than 3 wt.% Mn was doped into Co/AC catalysts. For example, the activity of 15Co5Mn/AC catalysts increased up to 50.9 mmol CO g Co<sup>-1</sup> h<sup>-1</sup>, while the selectivity of CH<sub>4</sub> increased unfortunately up to 27.3%.

As for the Cr-promoted catalysts, the addition of Cr could enhance the activity of Co/AC catalysts. It appears that the activity of 15Co3Cr/AC was the highest in Cr-promoted catalysts, which reached to 58.6 mmol CO g Co<sup>-1</sup> h<sup>-1</sup> that almost was equal to the level of 15Co/AC-S. Meanwhile, the selectivity of CH<sub>4</sub> also increased with the addition of Cr. Therefore, it could be concluded that the doping of various promoters and steam-pretreatment at high temperature could change the activity and the product distribution of Co/AC catalysts in FTS.

### 3.2. XRD measurement

Figures 1 and 2 demonstrate the XRD patterns of various used and passivated Co-based catalysts. The Co species existed in four kinds of compounds according to the XRD patterns, which included  $\alpha$ -Co, cubic Co, Co<sub>2</sub>C and Co<sub>3</sub>O<sub>4</sub> (figure 1). There appeared [100] and [101] for  $\alpha$ -Co species, [111] and [200] for cubic Co, [311] for Co<sub>3</sub>O<sub>4</sub> and there were three peaks belonged to Co<sub>2</sub>C species in the XRD patterns.

It is obvious that the apparent difference between 15Co/AC and 15Co/AC-S was whether there were the diffraction peaks of Co<sub>2</sub>C species. There were some strong peaks that attributed to Co<sub>2</sub>C species in the XRD pattern of 15Co/AC samples, while no Co<sub>2</sub>C species could be detected except for the peaks that ascribed to cubic Co species in 15Co/AC-S (see figure 1b). The Co particle sizes of used Co-based catalysts, the relative intensity of Co<sub>2</sub>C species to corresponding cubic Co species and the relative intensity of cubic Co to that in 15Co/AC are summarized in table 2. From the data shown in table 2, it was found that the Co metallic

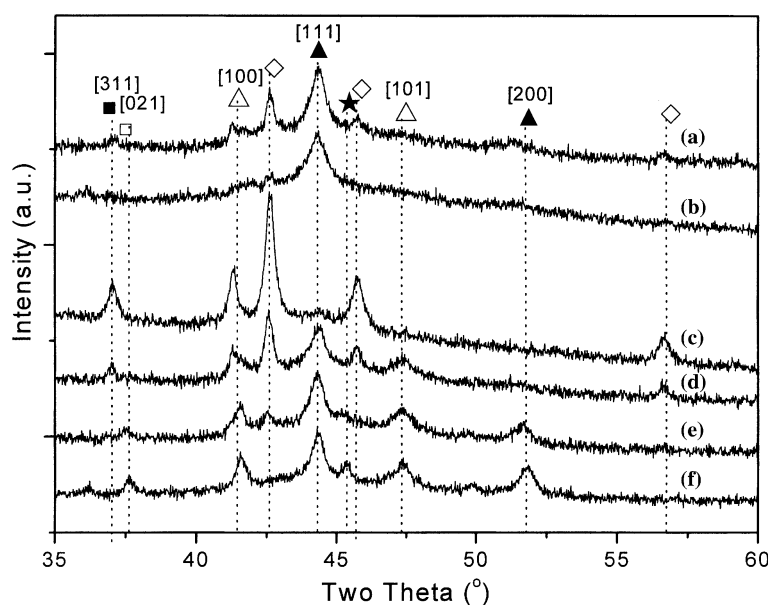


Figure 1. XRD patterns of used Co-based catalysts (a) 15Co/AC; (b) 15Co/AC-S; (c) 15Co1K/AC; (d) 15Co1Mn/AC; (e) 15Co3Mn/AC; (f) 15Co5Mn/AC. ■:  $\text{Co}_3\text{O}_4$ ; □: MnO; ▲: Cubic Co; △:  $\alpha$ -Co; ★:  $\text{Mn}_5\text{C}_2$ ; ◆:  $\text{Co}_2\text{C}$ .

particle size of 15Co/AC-S was bigger than that of 15Co/AC catalysts. Based on the results of CO hydrogenation and XRD measurements of 15Co/AC and 15Co/AC-S catalysts, it could be concluded that the increase of catalytic activity was mainly relative to whether existence of  $\text{Co}_2\text{C}$  species in Co-based catalysts. So it could be deduced that the formation of  $\text{Co}_2\text{C}$  species reduced the activity in FTS, which is due to the low density of metallic Co active sites and the decrease of accessible Co atoms available for F-T reaction [18].

Meanwhile, figure 1c shows that the Co species existed in the 15Co1K/AC catalyst majored in the

format of  $\text{Co}_2\text{C}$ ,  $\alpha$ -Co and  $\text{Co}_3\text{O}_4$ . It is appears that the XRD intensity of  $\text{Co}_2\text{C}$  species greatly increased when K was doped in 15Co/AC samples. Therefore, it could be extrapolated from above findings that low CO conversion of FTS was obtained over 15Co1K/AC catalysts. The low CO conversion of 15Co1K/AC catalysts further proven an inversion impact of  $\text{Co}_2\text{C}$  species formation on the performance of Co-based catalysts in F-T reaction. This was also the reason why steam-pretreatment of activated carbon and doping of K had an opposite effect on the activity of 15Co/AC catalyst in FTS.

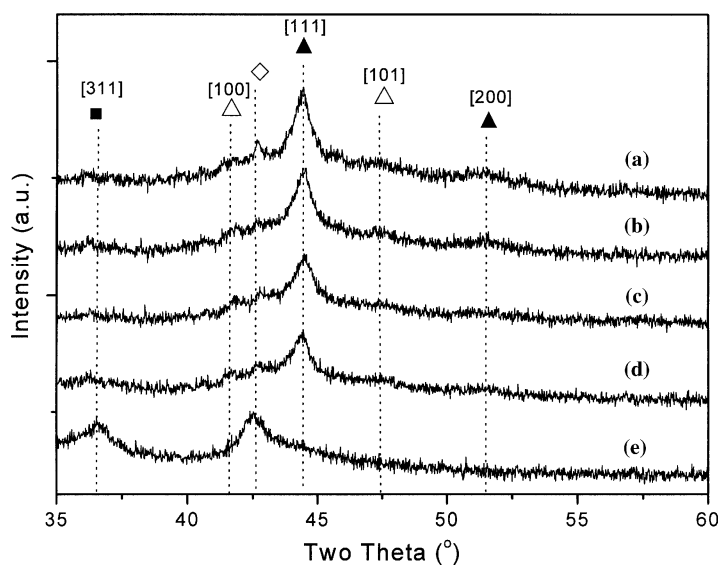


Figure 2. XRD patterns of used Cr-promoted catalysts and passivated catalyst (a) 15Co1Cr/AC; (b) 15Co3Cr/AC; (c) 15Co5Cr/AC; (d) 15Co7Cr/AC; (e) 15Co/AC-P. ■:  $\text{Co}_3\text{O}_4$ ; △:  $\alpha$ -Co; ▲: cubic Co; ◆:  $\text{Co}_2\text{C}$ .

For the XRD patterns of Mn-promoted catalysts, the relative intensity of the peaks belong to  $\alpha$ -Co [100] and [101], cubic Co [111] and [200] which shown in figure 1d–f increased while those of the peaks ascribed to  $\text{Co}_2\text{C}$  decreased with the amount of Mn doping. It is obvious from the data shown in table 2 that the ratio of the intensity of  $\text{Co}_2\text{C}$  species at  $2\theta=42.5^\circ$  to that of cubic Co [111] species at  $2\theta=44.3^\circ$  in 15Co1Mn/AC sample was larger than that of 15Co/AC catalysts, which caused the decrease of catalyst in F–T reaction. However, the diffraction peaks of  $\text{Co}_2\text{C}$  species almost disappeared when 5 wt.% of Mn was doped into 15Co/AC samples, consequently, CO conversion of 15Co5Mn/AC catalysts was the highest one in all

Mn-promoted catalysts. Therefore, the doping of Mn promoter could change the capability of  $\text{Co}_2\text{C}$  formation in Co/AC catalysts. In addition, it was found that the dispersion of Co particles in Co/AC catalysts decreased when Mn was doped into the Co-based catalysts.

A similar restraining effect of Cr on the formation of  $\text{Co}_2\text{C}$  species could also be observed in Cr-promoted Co/AC catalysts. The diffraction peaks of  $\text{Co}_2\text{C}$  at  $2\theta=42.5^\circ$  species disappeared when the loading of Cr addition reached more than 3 wt.% (see figure 2b–d). From the data shown in table 2, it was found that the Co particle sizes of Cr-promoted Co/AC catalysts first increased from 23.0 up to 63.4 nm when the amount of Cr doping reached 3.0 wt.%, then decreased from 63.4 down to 21.1 nm when 7.0 wt.% of Cr was doped into Co/AC samples. Concurrently, the activity of CO hydrogenation first enhanced from 28.4 up to 58.6 mmol  $\text{CO g Co}^{-1} \text{h}^{-1}$  when 3.0 wt.% was added into Co/AC catalysts, then descended from 58.6 to 54.5 mmol  $\text{CO g Co}^{-1} \text{h}^{-1}$  with the continuous increase of Cr loading up to 7.0 wt.% (see table 1).

$\text{Co}_2\text{C}$  species could also be found in the passivated 15Co/AC samples (figure 2e), which implied that the  $\text{Co}_2\text{C}$  species were formed during the reduction of catalysts at 623 K under hydrogen atmosphere. The temperature of 583–663 K was favorable to the formation of  $\text{Co}_2\text{C}$  species [19].

### 3.3. XPS measurement

Figure 3 shows the  $\text{C}_{1s}$  XPS spectra of used 15Co1K/AC and 15Co/AC-S samples. There were two peaks centered at 283.2 and 284.6 eV in the  $\text{C}_{1s}$  XPS spectra fitted using Gaussian method of 15Co1K/AC catalyst

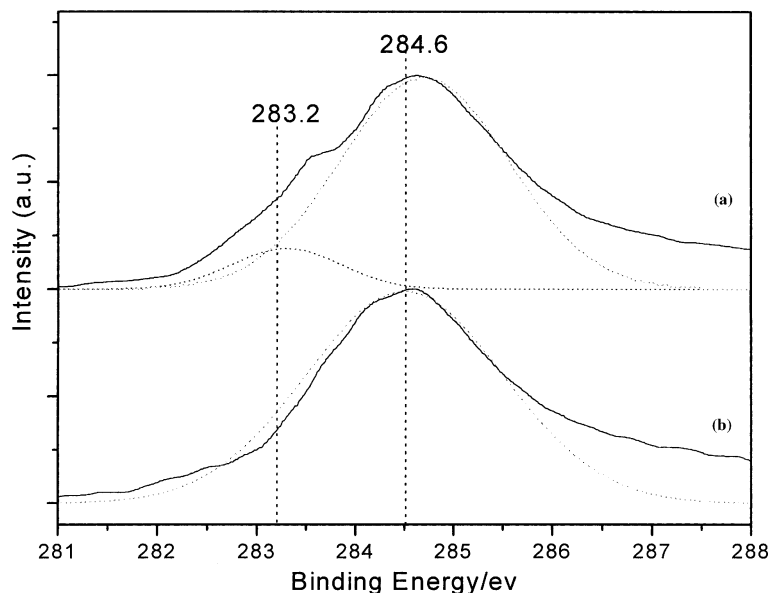


Figure 3.  $\text{C}_{1s}$  XPS spectra of used Co-based catalysts (a) 15Co1K/AC; (b) 15Co/AC-S.

Table 2

The Co particle sizes of catalysts and the ratio of the intensity of  $\text{Co}_2\text{C}$ /cubic Co and relative intensity of cubic Co species

Catalysts	Co particle size (nm)	Ratio of $\text{Co}_2\text{C}$ /cubic Co <sup>a</sup>	Relative intensity of cubic Co <sup>b</sup>
15Co/AC	23.0	0.76	1
15Co/AC-S	63.4	–	0.87
15Co1K/AC	–	∞	–
15Co1Mn/AC	23.1	1.22	0.68
15Co3Mn/AC	42.2	0.34	0.77
15Co5Mn/AC	36.2	–	0.77
15Co1Cr/AC	42.2	0.31	0.99
15Co3Cr/AC	63.4	–	0.85
15Co5Cr/AC	42.2	–	0.61
15Co7Cr/AC	21.1	–	0.59

<sup>a</sup>The ratio of the intensity of  $\text{Co}_2\text{C}$  at  $2\theta=42.5^\circ$  to that of the cubic Co [111] in the same catalyst.

<sup>b</sup>The ratio of the intensity of cubic Co [111] in Co-based catalysts and that in 15Co/AC catalysts.

(figure 3a). The peak at 283.2 eV corresponded to the binding energy of C<sub>1s</sub> in Co<sub>2</sub>C species, the peak at 284.6 eV attributed to that of carbon-carbon bonds [20]. It is obvious that C<sub>1s</sub> peak of Co<sub>2</sub>C species at 283.2 eV could not be observed in the 15Co/AC-S samples which shown figure 3b.

In summary, the evidence for the presentation of Co<sub>2</sub>C species formed during the reduction at 623 K in the Co/AC catalysts was obtained by XRD and XPS measurements, and the formation of Co<sub>2</sub>C species reduced the activity of CO hydrogenation over the Co-based catalysts. The doping of promoters, such as Mn and Cr, and pretreatment of the activated carbon with steam could restrain the formation of Co<sub>2</sub>C species, consequently, increase the activity of CO hydrogenation.

### Acknowledgements

The authors gratefully acknowledge the financial support by British Petroleum Corporation.

### References

- [1] S. Krishnamoorthy, A. Li and E. Iglesia, *Catal. Lett.* 80 (2002) 77.
- [2] H. Schulz, *Appl. Catal. A* 186 (1999) 3.
- [3] P. Dutta, N.O. Elbashir, A. Manivannan, M.S. Seehra and C.B. Roberts, *Catal. Lett.* 98 (2004) 203.
- [4] M.J. Keyserl, R.C. Everson and R.L. Espinoza, *Appl. Catal. A* 171 (1998) 99.
- [5] Y. Okamoto, K. Nagata, T. Adachi, T. Imanaka, K. Inamura and T. Takyu, *J. Phys. Chem.* 95 (1991) 310.
- [6] B. Jongsomjit, J. Panpranot and J.G. Goodwin, *J. Catal.* 204 (2001) 98.
- [7] R. Riva, H. Miessner, R. Vitali and G.D. Piero, *Appl. Catal. A* 196 (2000) 111.
- [8] M. Vob, D. Borgmann and G. Wedler, *J. Catal.* 212 (2002) 10.
- [9] Y. Brik, M. Kacimi, M. Ziyad and F. Bonzon-Verduraz, *J. Catal.* 202 (2001) 118.
- [10] J. Barrault, A. Chafik and P. Gallezot, *Appl. Catal.* 67 (1991) 257.
- [11] J. Barrault, A. Guilleminot, J.C. Achard, V. Paul-Boncour and A. Percheron-Guegan, *Appl. Catal.* 21 (1986) 307.
- [12] R.C. Reuel and C.H. Bartholomew, *J. Catal.* 85 (1984) 78.
- [13] A. Guerrero-Ruiz, A. Sepúlveda-Escribano and I. Rodríguez-Ramos, *Appl. Catal. A* 120 (1994) 71.
- [14] T. Wang, Y.J. Ding, J.M. Xiong, W.M. Chen, Z.D. Pan, Y. Lu and L.W. Lin, *Stud. Surf. Sci. Catal.* 147 (2004) 349.
- [15] W.P. Ma, Y.J. Ding and L.W. Lin, *Ind. Eng. Chem. Res.* 43 (2004) 2391.
- [16] J.M. Xiong, Y.J. Ding, T. Wang, W.M. Chen, L. Yan and H.J. Zhu, *Petrochem. Technol.* 33 (2004) 203.
- [17] T. Wang, Y.J. Ding, J.M. Xiong, L. Yan, W.M. Chen and L.W. Lin, *Petrochem. Technol.* 33 (2004) 200.
- [18] E.K. Coulter and A.G. Sault, *J. Catal.* 154 (1995) 56.
- [19] G.G. Volkova, T.M. Yurieva, L.M. Plyasova, M.I. Naumova and V.I. Zaikovskii, *J. Mol. Catal. A-Chem.* 158 (2000) 389.
- [20] H. Wang, S.P. Wong, W.Y. Cheung, N. Ke, W.F. Lau, M.F. Chiah and X.X. Zhang, *Mat. Sci. Eng. C* 16 (2001) 147.